International Journal of Hydrogen Energy 89 (2024) 952–963

Contents lists available at ScienceDirect

International Journal of Hydrogen Energy

journal homepage: www.elsevier.com/locate/he

Hydrogen enrichment in methanol SI engine at varying injection timing during compression stroke

S.N. Iyer *, D.N. Rrustemi, L.C. Ganippa, T. Megaritis

Department of Mechanical and Aerospace Engineering, Brunel University London, Uxbridge, London, UB8 3PH, UK

ARTICLE INFO

Keywords:
Hydrogen
Injection timing
Methanol
Mixing
Spark-ignition engine

ABSTRACT

This study investigates the effect of hydrogen enrichment in a direct-injected methanol-fuelled SI engine, with combustion and emission performance analysed by varying the methanol injection timing from 150° to 60° CA bTDC. A three-dimensional computational fluid dynamic model of the hydrogen-enriched methanol engine was developed to predict the engine performance, in-cylinder, and emission characteristics. The numerical model was solved using three-dimensional Reynolds-Averaged Navier Stokes, the RNG k-epsilon model for turbulence, the O'Rourke and Amsden sub-model for heat transfer, the extended Zeldovich mechanism for nitric oxide emissions, and the Hiroyasu-NSC model for soot emissions. The results indicated that retarding the injection timing resulted in a decrease in the indicated specific CO and soot emissions along with a rise in the indicated specific NOx emissions. Furthermore, hydrogen enrichment with methanol enhanced the hydroxyl radical concentration, reduced the combustion duration, reduced also the indicated specific CO and soot emissions while increasing the indicated specific NOx emissions. The study indicates that hydrogen enrichment could extend the late injection timing limit of methanol by enhancing fuel-air mixing, which improves and controls the combustion process more effectively.

1. Introduction

The utilisation of fossil fuels for power generation contributes significantly to environmental pollution and greenhouse gas emissions. Most of major stationary power generation sectors are exploring into renewable alternative fuels to power internal combustion engines to address the challenges of CO_2 emissions [1,2]. Bio-methanol is one of the promising low carbon alternative fuel for road and water transport because of its convenience in production from waste and biomass. Countries around the world are developing technical pathways and infrastructure to produce methanol from carbon dioxide through hydrogenation [2–6]. Methanol also has its advantages due to its easy storage, transportation, substantial availability, higher octane number and its resistance to knocking that enables higher compression ratios, and therefore for higher efficiency [7]. Furthermore, methanol has higher heat of vaporization (as shown in Table 1) contributes to charge cooling which delays the onset of knocking with better combustion and emission performance [7,8]. Compared to diesel and gasoline, methanol could be operated under leaner conditions due to its higher laminar burning velocity [9]. Therefore experimental investigations have been performed to study the effects of methanol addition in diesel engines, this has resulted in an improvement in brake thermal efficiency, along with a reduction in CO and soot emissions [10]. Similarly, methanol enriched gasoline fuelled spark ignited engine have also shown a benefit of reduction in CO emissions [6,11].

In addition to renewable methanol, hydrogen is also considered as a promising alternative zero carbon fuel with better combustion characteristics, high calorific value, and environmental advantage when compared to conventional fuels [4,12]. The experimental investigation on hydrogen enrichment in natural gas engines has revealed that the misfire limit can be extended under lean operating conditions [13–15]. Similarly implementation of hydrogen to methanol fuelled engines enhances combustion and emissions performance [16–20]. Hydrogen enriched methanol engine has shown to improve the engine performance and reduce the CO and unburned hydrocarbon compared to other alternative fuels [21]. As hydrogen enrichment with methanol offers stable combustion due to methanol's higher-octane rating and hydrogen's wide flammability limits, compared to hydrogen addition to gasoline or natural gas in spark-ignition engines [22]. The study conducted by Ref. [23] has shown that hydrogen enrichment in methanol under stoichiometric condition reduces emissions such as CO and HC but the

* Corresponding author.
E-mail addresses: Subramanian.Narayanaiyer@brunel.ac.uk (S.N. Iyer), Dardan.Rrustemi@brunel.ac.uk (D.N. Rrustemi), Lionel.Ganippa@brunel.ac.uk (L.C. Ganippa), Thanos.Megaritis@brunel.ac.uk (T. Megaritis).

https://doi.org/10.1016/j.ijhydene.2024.09.297
Received 1 August 2024; Received in revised form 12 September 2024; Accepted 22 September 2024
Available online 2 October 2024

Nomenclature

3D	Three-dimensional
AFR	Air to fuel ratio
CA	Crank angle
CA10	10% mass fraction burned
CA10-90	Combustion duration
CA90	90% mass fraction burned
CFD	Computational fluid dynamics
CH_3OH	Methanol
CO	Carbon monoxide
CR	Compression ratio
α	Hydrogen addition (%)
H_2	Hydrogen
IMEP	Indicated mean effective pressure
IT	Injection timing
MAP	Manifold air pressure (kPa)
m_{air}	Mass of air (kg)
m_{H_2}	Mass of hydrogen (kg)
m_{CH_3OH}	Mass of methanol (kg)
N	Engine speed (RPM)
NO	Nitric oxide
NOx	Oxides of Nitrogen
NSG	Nagel Strickland-Constable
OH	Hydroxyl radical
RANS	Reynolds-Averaged Navier-Stokes
RNG	Renormalization group
SI	Spark ignition
ST	Spark timing
AF_{H_2st}	Stoichiometric air to fuel ratio of hydrogen
AF_{CH_3OHst}	Stoichiometric air to fuel ratio of methanol
TDC	Top dead center
V_{H_2}	Volumetric flow rates of hydrogen (kg/s)
V_{air}	Volumetric flow rates of methanol (kg/s)
bTDC	Before top dead center
d_{max}	Largest standard deviation (kPa)
k-ε	K-epsilon
Φ	Equivalence ratio
ε	Standard error (%)
λ	Excess air ratio

Table 1
Properties of methanol and hydrogen [28].

Properties	Methanol	Hydrogen
Formula	CH_3OH	H_2
Molecular mass (kg/mol)	32	2
Density (kg/m^3)	790	0.0899
Octane number	111	20–30
Latent heat of vaporization (kJ/kg)	1110	–
Stoichiometric ratio	6.5	32
Laminar flame velocity (m/s)	0.523	2.912
Lower calorific value (MJ/kg)	19.6	120.1

NOx emissions increased due to an increase of the peak in-cylinder combustion temperature. The increase of NOx emission have also be addressed by extending the lean limits of the methanol combustion through hydrogen enrichment which has shown a reduction in peak in cylinder pressure and temperature [18]. Under higher engine speed enrichment of hydrogen to a methanol SI engine resulted in IMEP increase, but it also increased soot and NOx emissions [24]. Hydrogen addition to a methanol engine resulted in increase in the soot emissions because the higher hydrogen addition because high concentration of H-ion cause surface oxidation reaction of the soot. Hydrogen addition could slow prevent the soot oxidation due to the influence in the combustion temperature and chemical reaction. Enrichment of hydrogen can also slow down the formation polycyclic aromatic hydrocarbon which would contribute to soot formation [25]. Moreover, for lower engine speed of 1200 rpm the IMEP decreased with adding hydrogen due to weak airflow motion entering the cylinder [26]. As increasing the hydrogen addition to a methanol SI engine can reduce volumetric efficiency, resulting in a slower flame propagation speed [27].

The importance on injection timing on mixture preparation have been corroborated in Ref. [29]. The injection timing of methanol play a crucial role in enhancing fuel droplet dispersion, evaporation, mixing an attainment of a homogeneous mixture in controlling the combustion and emission formation under wider range of equivalence ratios [1,30,31]. Injecting fuel too early results in fuel droplet impinging on piston crown and cylinder wall, whereas delayed injection could reduce the time for effective fuel-air mixing [30,32,33]. A study conducted on varying the injection timing in an ethanol-fuelled direct injection engine, has shown that by advancing the injection timing during the intake process within the range of 240–300 °CA bTDC led to a small reduction in the indicated mean effective pressure (IMEP) at medium load operation. However, when the injection timings were advanced further, between 300 and 330 °CA bTDC, an increase in IMEP of 1.34% at medium load and 1.51% at low load conditions was observed. Additionally, advancing the injection timing during the compression stroke from 60 to 80 °CA bTDC resulted in an increase of IMEP by less than 1% [34]. It has been shown that by injecting multi-component surrogate fuel in gasoline engine at an injection timing of 290 °CA bTDC reduced the soot emissions but this also led to the formation of fuel film on the piston top surface due to low volatility components present in the fuel [35]. A numerical study on the injection timing variation of during the intake stroke in a gasoline direct injection engine has shown that by advancing injection timing to 300 °CA bTDC the emissions reduced due to increase in homogeneity for earlier injection timings [22,23]. According to the study conducted by Ref. [19] on a methanol direct injection has shown that varying the ignition timing from 13 °CA to 21 °CA bTDC resulted in an increase in CO, HC, NOx emissions and a reduction in thermal efficiency, whilst advancing the injection timing resulted in a rise in hydrocarbon and NOx emissions and a reduction in CO emissions. This has been demonstrated further by injecting blend of n-butanol and gasoline at different proportion in the intake port led to an increase in the hydrocarbon (HC) emission, particularly when fuel mixture was injected at 64 °CA before the inlet valve opening [36]. The existing works [27,37–41] reveals that there is a notable gap in understanding the effect of injection timing of methanol with hydrogen enrichment in engines.

This study employs a computational fluid dynamics (CFD) model to explore the impact of varying the in-cylinder injection timings of methanol for different amount of hydrogen addition through the intake port. This research examines the effect of methanol injection at 150, 110, 80, and 60 °CA bTDC during the compression stroke when the hydrogen concentration in the engine was varied from 0 to 12%. Then late injection limit on mixing and combustion performance of neat methanol as well as hydrogen enrichment operation have been considered for different spark timing. This study explores salient parameters such as in-cylinder mixing, combustion characteristics, formation of gaseous and soot emissions for the above-mentioned operating conditions.

2. Methodology

2.1. Operating conditions

The initial and boundary conditions of the 3D CFD hydrogen enriched methanol SI engine model are directly linked to the experimental data of [42]. The values for the injection timing, spark timing and hydrogen additions are detailed in Table 2. All simulations were conducted by fixing the operating conditions of injection pressure at 110 bar, equivalence ratio at 0.71, manifold air pressure at 90 kPa, compression ratio at 9.6 and the engine speed at 1200 rpm.

2.2. Hydrogen addition

The hydrogen was added to methanol as a volume fraction of the intake air, defined as:

$$\alpha = \frac{V_{H_2}}{V_{air} + V_{H_2}} \quad (1)$$

where V_{H_2} and V_{air} are the volumetric flow rates of hydrogen and air, respectively. The excess air ratio of the dual-fuel methanol/hydrogen was calculated as:

$$\lambda = \frac{m_{air}}{m_{H_2} AF_{H_2st} + m_{CH_3OH} AF_{CH_3OHst}} \quad (2)$$

where m_{air}, m_{H_2} and m_{CH_3OH} are the masses of air, hydrogen and methanol, respectively. AF_{H_2st} and AF_{CH_3OHst} are the stoichiometric ratios, defined as 34 and 6.5, respectively.

2.3. Combustion model

A 3D model of hydrogen-enriched lean burn methanol SI engine including the intake and exhaust port was built to predict the combustion and emission characteristics. The basic grid size for the 3D model was 4 mm. The in-cylinder region was refined to a mesh size of 1 mm during the combustion and gas exchange process. Finally, a finer embedding of 0.5 mm was applied around the injector and the spark plug to capture the flame characteristics such as: kernel formation its growth, and development as shown in Fig. 1a and b. This was the optimum mesh refinement used in this work, further mesh refinement did not result in any significant improvement in predicted results. The spark timing and spark energy were replicated by the source/sink modelling. This approach was used to replicate the arc phase and glow phase of the spark, with a duration of 0.5 °CA for the arc phase and a duration of 8 °CA for the spark. The adaptive mesh refinement (AMR) was applied automatically by the solver, and the mesh was refined based on the local gradient of temperature and velocity.

The computational fluid dynamics (CFD) solver, Converge [43], was used to solve the three-dimensional Reynolds-Averaged Navier Stokes (RANS) equations and the turbulence inside the combustion chamber was simulated using RNG k-ε model [44]. The O'Rourke and Amsden heat transfer sub-model was applied and for combustion investigations, SAGE a detailed chemistry solver was used to calculate the reaction rates of all elementary reactions of the methanol/hydrogen combustion mechanism [45,46]. This mechanism, consist of 20 elementary reversible reactions, which has been validated across a wide range of experimental data.

The NOx emission formation is primarily dependent on in-cylinder temperature and equivalence ratio of the mixture, extended Zeldovich mechanism have been used to calculate the thermal NO formation under methanol combustion environment. The extended Zeldovich mechanism was incorporated into the CFD model to compute NO emissions, and the Hiroyasu-NSC soot model was employed to assess soot at different equivalence ratios, spark timings, and hydrogen addition. The soot processes were predicted using the Hiroyasu empirical model to calculate soot formation and Nagel Strickland-Constable (NSG) model to calculate the soot oxidation process [47].

Table 2
Simulation conditions.

Injection timing [°CA bTDC]	150	120	80	60
Spark timing [°CA bTDC]	20	20	20	20–4
Hydrogen addition [increments of 3%]	0–12	0–12	0–12	0–12

2.4. Model validation

The in-cylinder pressures at different equivalence ratios, spark timings, and hydrogen additions were validated using the published experimental data of [42]. The engine specifications of their single-cylinder hydrogen enriched methanol SI engine are shown in Table 3.

Fig. 2 shows the validation of in-cylinder pressure data for neat methanol SI engine operation at 1200 rpm with fuel injection timing of 80 °CA bTDC, at an equivalence ratio of 0.83, spark timing of 28 °CA bTDC and a compression ratio of 9.6. It can be observed that the in-cylinder pressure predictions were satisfactory for the chosen experimental operating condition of the engine. The largest standard deviation, d_{max}, was 119 kPa during the compression process, and the maximum error, ε, was within 2%, which was within the cycle-to-cycle variation of the experimental data. Fig. 2 also compares experimental and simulated results for the in-cylinder pressure at an injection timing of 80°CA bTDC of methanol with 6% hydrogen addition at an equivalence ratio of 0.71 for a spark timing of 12 °CA bTDC. The Comparison of results for the numerical in-cylinder pressure and experimental data are satisfactory for the selected operating condition. Quantitative differences between the simulated and experimental data were analysed, which resulted in a standard error ε, of ~1% and a maximum standard deviation, d_{max}, of 40 kPa these values are within the range of cyclic variations.

3. Results and discussion

3.1. In-cylinder pressure

The injection timing effect on the in-cylinder pressure variations for neat methanol SI engine at an injection timing of 150, 110 and 80 °CA bTDC are presented in Fig. 3. It can be observed that the in-cylinder pressure did not vary significantly for methanol injection timing between 80 and 110 °CA bTDC, where the magnitudes of in-cylinder peak pressures were 5.38 MPa and 5.28 MPa, respectively. But, with the advancement of injection to 150 °CA bTDC, the peak pressure reduced by 17% compared to the case when methanol was injected at 80 °CA bTDC. This was due to the accumulation of rich stratified regions of fuel-air mixture within the chamber during compression which also causes a drop in OH concentration during the combustion process that will later be discussed in Figs. 6–9.

Fig. 4 represents the variation of in-cylinder pressure for varying percentages of hydrogen addition (0–12%) at an injection timing of 80 °CA bTDC when maintained at an equivalence ratio of 0.71. It can be seen that by increasing the hydrogen addition up to 9% the combustion rate was enhanced due to higher flame speeds of hydrogen and its adiabatic flame temperature compared to neat methanol, similar effects were also observed in Ref. [48]. The in-cylinder pressure rise can be related to the advancement of the position of peak cylinder pressure by 5 °CA with 3% hydrogen and by 6 °CA with 9% hydrogen compared to 0% hydrogen addition. Meanwhile, the peak in-cylinder pressure increased by 6.7% and 7.0% for 3% hydrogen addition and 9% hydrogen addition respectively compared to pure methanol operation. The benefit of hydrogen enrichment on the combustion characteristics was not observed for 12% hydrogen addition. Where the peak in-cylinder

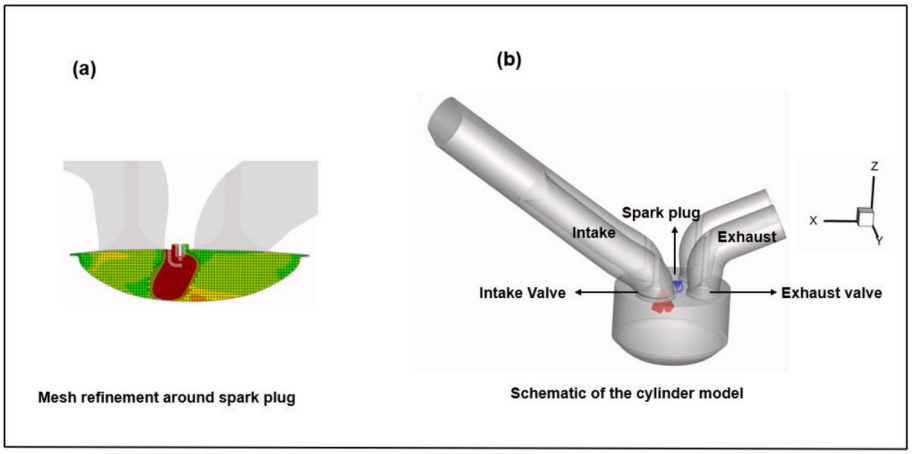

Fig. 1. a) Adaptive mesh refinement around the spark and b) schematic of the in-cylinder model.

Table 3
SI engine specifications used in this study.

Characteristics	Values
Bore [m] x stroke [m]	0.0825 x 0.0842
Displacement volume [m^3]	0.001798
Compression ratio [−]	9.6
Speed [rpm]	1200

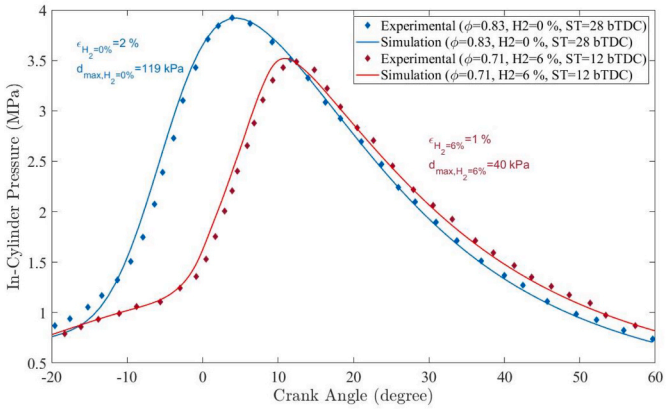

Fig. 2. In-cylinder pressure of hydrogen enriched methanol SI engine, experimental values of [42] are presented as symbols, simulation results are presented as solid line (MAP = 90 kPa, CR = 9.6, N = 1200 rpm, IT = 80 °CA bTDC).

pressure reduced compared to 9% hydrogen addition. This may be associated with lower volumetric energy density of hydrogen which at higher percentages could result in lower overall energy content of the mixture inside the cylinder which was also noticed in Ref. [49].

Fig. 5 presents the simulated peak in-cylinder pressure values at different injection timings, with hydrogen additions ranging from 0 to 12%, at a fixed spark timing of 20°CA bTDC. The peak pressure was highest when methanol was injected at 80°CA bTDC, while the peak cylinder pressure was relatively lower at 150°CA for various levels of hydrogen addition (0%, 3%, 9%, 12%) with methanol. As can be seen from Figs. 3 and 5, the injection timing of 110°CA and 80 °CA bTDC did not have much impact on peak in-cylinder pressure for neat methanol as well as for 3%, 9% and 12% hydrogen addition, the difference was in the order of 1.5% greater for injection timing of 80 °CA bTDC. The data presented in Fig. 5 reveal that for the considered injection timings of 150, 110 and 80 °CA bTDC, the peak cylinder pressure increased with hydrogen addition and thereafter tends to decrease with 12% hydrogen

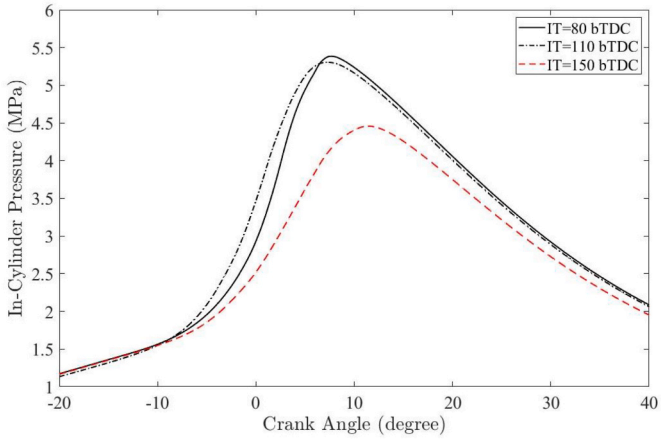

Fig. 3. Results for in-cylinder pressure of neat methanol at injection timings of 150, 110 and 80 °CA bTDC (Φ = 0.71, CR = 9.6, MAP = 90 kPa, N = 1200 rpm, ST = 20°bTDC).

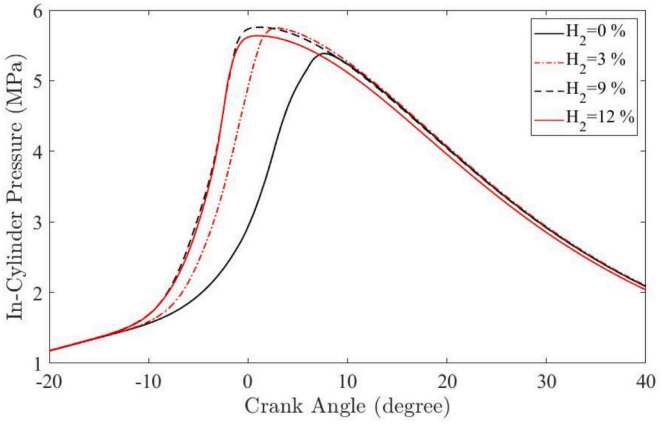

Fig. 4. Results for in-cylinder pressure with various hydrogen additions of 0%, 3%, 9% and 12% at fixed injection timing of 80 °CA bTDC,at a spark timing of 20 °CA bTDC (Φ = 0.71, CR = 9.6, MAP = 90 kPa, N = 1200 rpm).

injection. But when methanol was injected late at 60 °CA bTDC, the peak pressure was observed to be higher for 12% hydrogen addition when compared to 9% hydrogen addition. The mixing time was significantly reduced, no combustion occurred for neat methanol and for 3% hydrogen addition but combustion was initiated with the addition of 9%

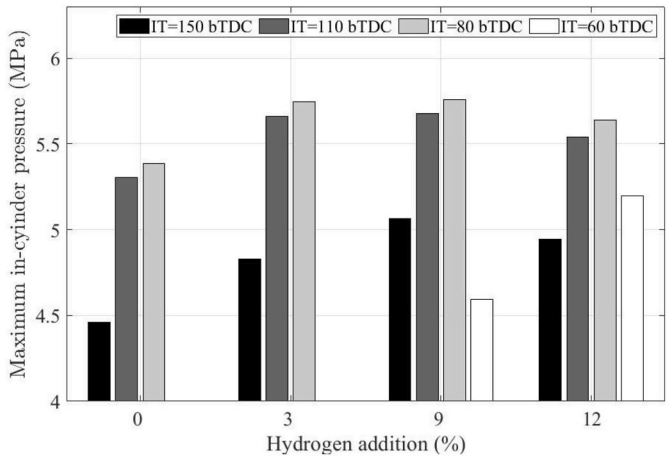

Fig. 5. Maximum in-cylinder pressure values for different hydrogen additions at different injection timings (ST = 20 °CA bTDC, Φ = 0.71, CR = 9.6, MAP = 90 kPa, N = 1200 rpm).

hydrogen. The peak pressure was observed to be higher for 12% hydrogen addition when compared to 9% and this could be due to hydrogen having faster flame propagation that enhanced combustion, particularly during late injection when the mixing time was relatively inadequate compared to earlier injection events.

3.2. In-cylinder mixing

Injection timing is a crucial parameter that controls in-cylinder mixing and combustion, the impact of early and late injection timings on the local equivalence ratio of the charge in the cylinder just before the occurrence of spark at 20 °CA bTDC are presented in Fig. 6 for various injection timing of 150, 110, 80, and 60 °CA bTDC. The injection of methanol at 150 °CA bTDC resulted in an accumulation of fuel on one side of the cylinder as shown in Fig. 6. The presence of relatively higher fuel concentration on the piston crown and cylinder wall towards the side of intake valve was noticed in the x-z and x-y plane, which suggests the occurrence of fuel impingement on cylinder wall due to the location of injector, and the associated spray-air interations. During compression process the tumble motion caused the fuel droplets to be transported to one side of the cylinder.This leads to an asymetric distribution of richer mixture at the later stages of the compression stroke, similar kind of fuel distribution patterns have been observed in Ref. [30]. When the start of injection was delayed from 150 to 100 or 80 °CA bTDC, a reduction in the uneven distribution of fuel-air mixture at the later stages of the compression stroke was observed for neat methanol and also for cases with hydrogen addition. Injecting methanol later then 80 °CA bTDC resulted in very ultra lean mixtures in the regions surrounding the spark plug as can be seenin Fig. 6 for injection at 60 °CA bTDC case. The differences in fuel-air mixture distribution in the chamber closer to the initiation of spark for early and later injection timings could be due to maintaining the same magnitude of 110 bar injection pressure. This led to wall impingement,fuel film formation that effects evaporation and mixing for early injection timing of 150 °CA, whilst this effect was minimised for later injection timings and similar observations have been reported in Refs. [31,50,51]. The effect of in-cylinder flow field on mixing and transport of injected fuel spays during the compression stroke for different injection timings (150 °CA bTDC, 110 °CA bTDC and 80 °CA bTDC) of neat methanol and 9% hydrogen addition are presented in Fig. 7. The simulation analysis revealed that during the early stages of the compression process two counter rotating vortices were observed, one on either sides of the cylinder when viewed in the x-y plane. This is in line with [29]. When methanol was injected at 150 °CA bTDC, it could be observed that during the compression stroke at 69 °CA bTDC, the velocity field at the left side of the cylinder transports the fuel-air fuel mixture towards the wall and to the cylinder head as can be seen at 57 °CA bTDC. Subsequently, at a later phase of the compression stroke at 20 °CA bTDC a rich fuel-air mixture accumulated below the intake valve region in the cylinder head as shown both in Figs. 6 and 7. When the injection time was retarded to 110 °CA bTDC, the accumilation of rich concentration of fuel-air mixture that was observed at 150 °CA bTDC injection timing towards the left side of the cylinder wall was reduced significantly at 69 °CA bTDC, 57 °CA bTDC and 20 °CA bTDC due to relatively improved evaporation and mixing. Also, in Fig. 7, a thin film of rich fuel mixture was formed at 69 °CA bTDC on the right side of piston crown, which subsequently vaporised and mixed by the counter rotating vortices. Futhermore, when the methanol injection timing was retarded futher to 80 °CA bTDC, a rich mixture was observed at the center of the piston bowl during upward motion at 69 °CA bTDC due to spray tip impingment on the piston. Later at 57 °CA bTDC, the fuel-rich regions were transported by the counter rotating vortices towards the left side of the piston bowl to mix further and to form a uniform mixture in the vicinity of the spark plug. Retarding the fuel injection timing to 80 °CA bTDC in comparison to injection timings at 150 °CA bTDC and 110 °CA bTDC resulted in a favourable interaction between the injected methanol sprays and charge motion, which resulted in a uniform distribution of mixture at the time of initiation of spark. The addition of hydrogen to methanol resulted in a decrease in the accumulation of rich fuel-air mixture on the left side of the cylinder wall, compared to pure methanol. Specifically, at an injection timings 150 °CA bTDC and 110 °CA bTDC, as can be seen in Fig. 7.During the compression process at 69 °CA bTDC, 57 °CA bTDC, and 20 °CA bTDC an enhanced uniformity of fuel-air mixing was observed for 9% of hydrogen addition, this improved mixing may be attributed to Ref. [52]. to maintaining a global equivalence ratio of 0.71,therefore the quantity of methanol fuel droplets had to be reduced when hydrogen was added. Reducing the amount of fuel droplet may also reduce the fuel film formation. Additionally, the presence of hydrogen also contribute to enhanced mixing and combustion [29,52,53].

For the later injection timing of 60 °CA bTDC, combustion did not initiate for neat methanol and also for 3% hydrogen addtion, this was mainly due to an inadequate time to forma rective mixture in the region surrounding the spark plug as seen in Fig. 8. But, when the hydrogen addtion was increased to 9% and 12%, the charge was ignited for the late methanol injection timing of 60 °CA bTDC. The increase in hydrogen addition contributed to the development of a flamable mixture near spark plug that initiated flame due to its wider flammability and higher flame speed compared to methanol. In order to explore the residence time effects on mixing during late injection, simulations were conducted for neat methanol operation at the 60 °CA bTDC injection timing by retarding the spark timing from 20 °CA bTDC to 4 °CA bTDC as shown in Fig. 8. The mixture distribution of methanol with air in the cylinder just before the initiation of spark showed that by delaying the spark timing from 20 to 4 °CA bTDC promoted mixing that led to a mixture homogenity near spark plug and initiation of flame. However incresing the amount of hydrogen also enhanced ignition and combustion performance by extending the injection timing limits which could eventually could increase the stability of ignition,combustion and improved thermal efficiency of and improved methanol/hydrogen SI engine [54].

3.3. OH radicals

Hydrogen addition to methanol helps to promote the generation rate of radicals such as O, H and OH during the oxidation process of methanol [20]. The hydroxyl radicals play a crucial role in influencing the speed of the chemical reaction and the corresponding increase of the in-cylinder temperature. In Fig. 9, the OH radical formation was explored with respect to crank angle for different injection timings (150 °CA, 110 °CA, and 80 °CA bTDC) and various hydrogen addition levels (0%, 3%, 9%,

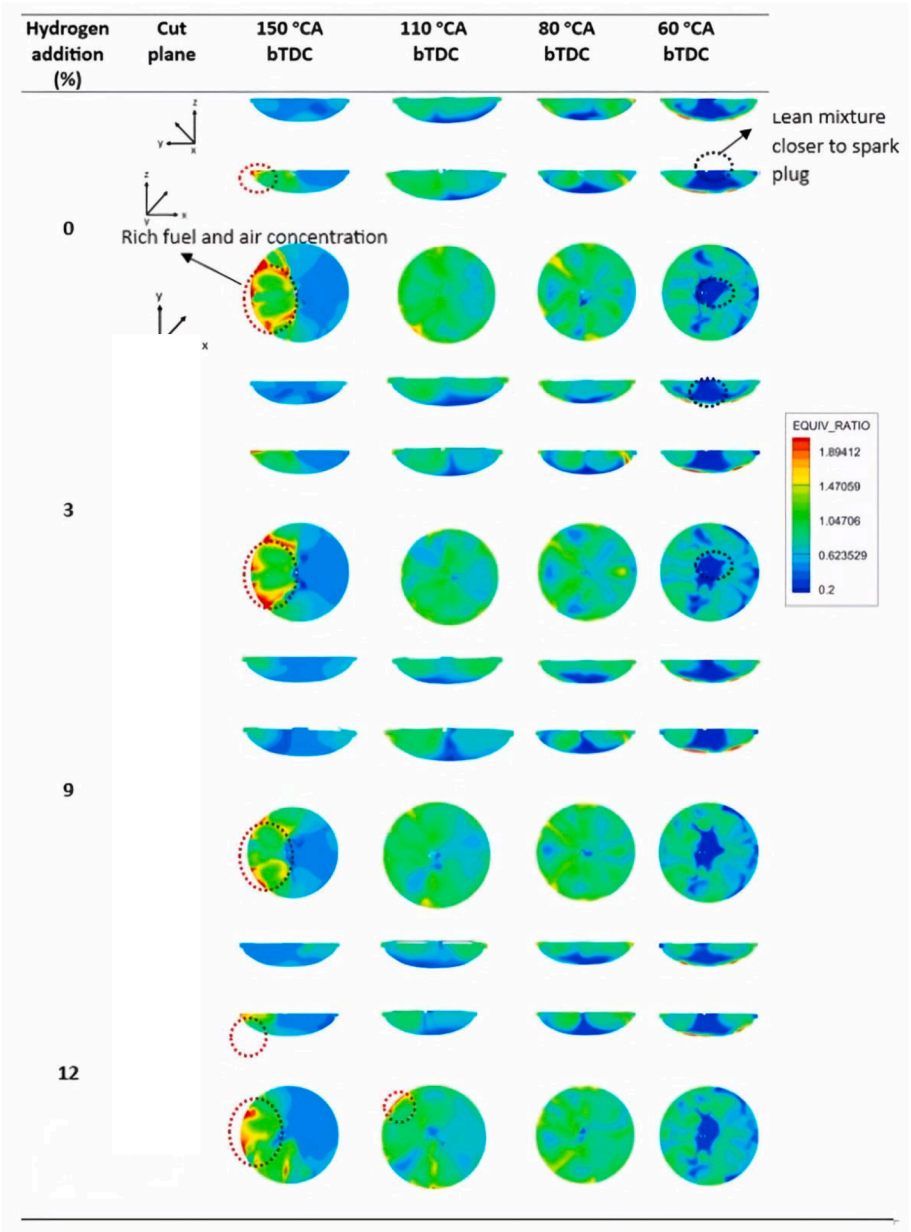

Fig. 6. Comparison of in-cylinder mixing for various hydrogen additions (0, 3, 9 and 12%) and injection timings (150, 120, 80 and 60 °CA bTDC) just before the initiation of spark at 20 °CA bTDC.

12%) for a constant spark timing of 20 °CA bTDC. The results showed that the effect of retarding the fuel injection timing from 150 °CA bTDC to 110 °CA bTDC and 80 °CA bTDC for neat methanol caused the peak value of OH to occur about 4 °CA earlier, with an associated increase in the peak OH concentration of 135.25% and 165% compared to injection of methanol at 150 °CA bTDC due to increase in homogeneity of charge discussed Figs. 6–8. The presence of rich stratified regions of fuel-air mixture at the vicinity of spark at 150°CA bTDC could have reduced the intensity of combustion as seen by delaying the formation of OH formation of OH radical during the combustion process. The difference between the initiation of OH formation and its peak are consistent with combustion duration shown in Fig. 10. Moreover, for the case of hydrogen addition greater than 3%, the value of peak OH occurred 4 °CA and 8 °CA earlier for an injection timing of 110 °CA and 80 °CA bTDC compared to 150 °CA bTDC. For 9% and 12% hydrogen addition, retarding the injection timing form 150 °CA to 110 °CA and 80 °CA led to a 65.28% and 81.94% increase in peak OH formation. Then OH was initiated quicker by retarding the injection timing at higher hydrogen addition, due to better quality mixing. For the case of 3% hydrogen addition, compared, retarding the injection timing to 150 °CA bTDC resulted in an increase of up to 82.11% and 88.36% in the peak value of OH for 110 °CA and 80 °CA bTDC, respectively. Increasing hydrogen addition also resulted in an increase in peak OH formation during the combustion process. This is due to hydrogen having higher flame speed that helps in fast oxidation process leading to an increase in OH radical concentration in the high temperature flame front and the associated high activation energy during combustion.

3.4. Combustion duration

The combustion duration is defined as the crank angle interval required to burn methanol/hydrogen mixture, from the start of flame development at CA10 to the end of flame propagation at CA90. In this study the combustion duration was calculated by considering the crank

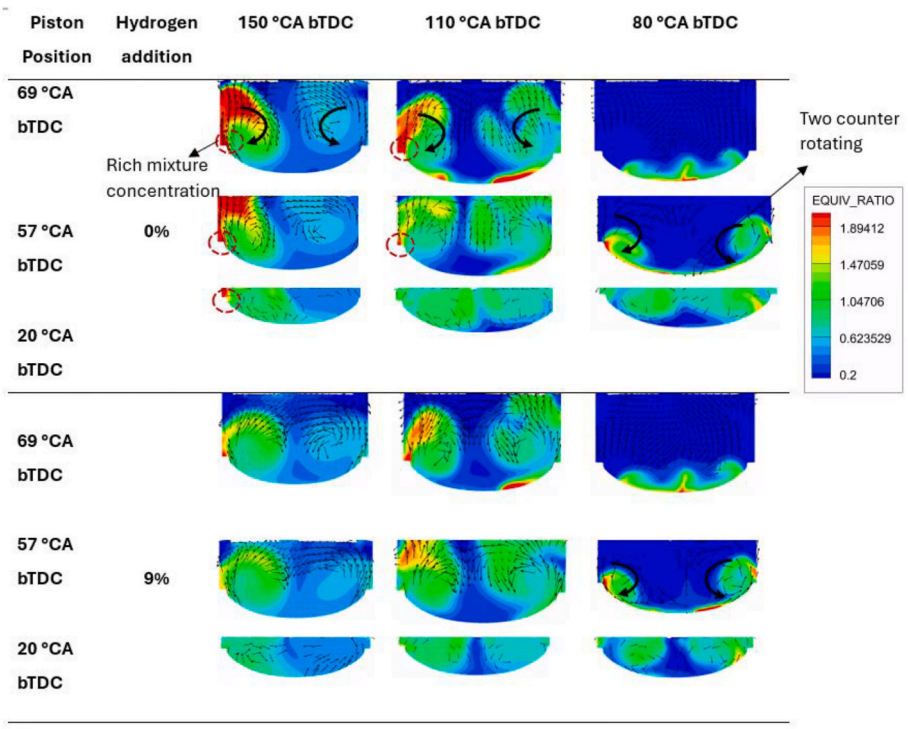

Fig. 7. Effect of velocity field distribution associated to in-cylinder mixing during the compression process for neat methanol and 9% hydrogen additions at injection timings (150, 110 and 80 °CA bTDC).

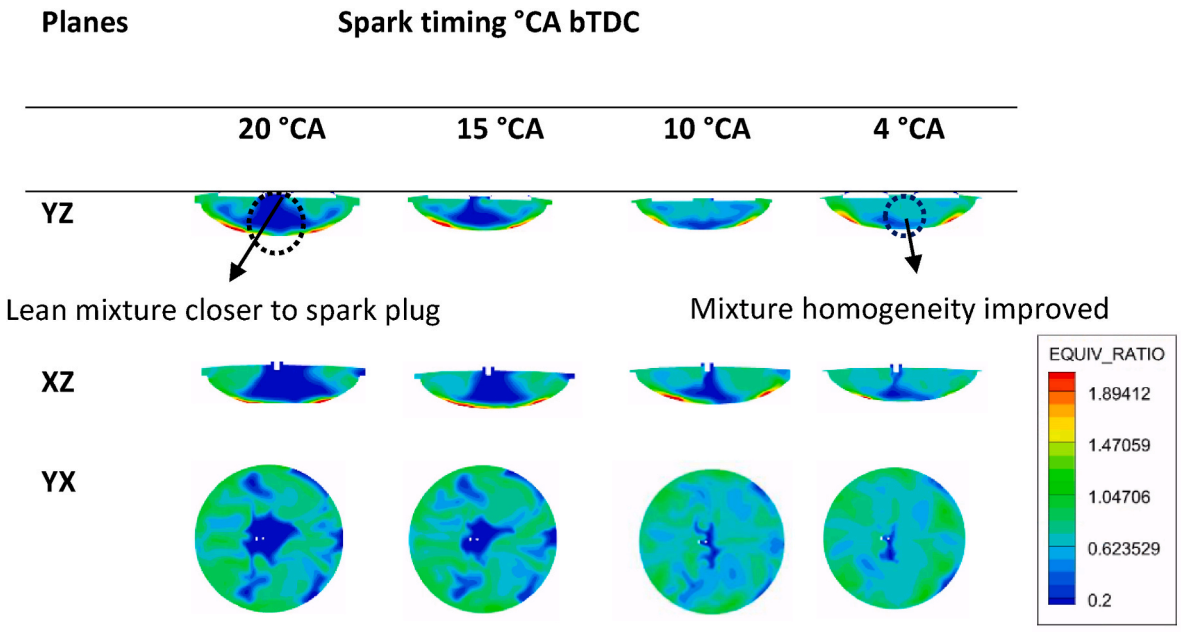

Fig. 8. In-cylinder mixing around the spark plug for different spark timing for pure methanol for 60 °CA bTDC injection timing.

angle difference between CA10 and CA90 values of the integrated apparent heat release rate. Fig. 10 represents the combustion duration (CA10-90) for the injection timings of 150 °CA, 110 °CA and 80 °CA bTDC of methanol with 0%, 3%, 9% and 12% hydrogen addition. Combustion duration reduced when the injection timing was retarded from 150 °CA bTDC to 80 °CA bTDC under all conditions. Delaying the injection timing of methanol from 150 °CA bTDC to 110 °CA bTDC resulted in a decrease in combustion duration by 6.29% for pure methanol, a reduction of 39.03%, 32.08%, and 27.93% was observed for methanol with 3%, 9%, and 12% hydrogen addition, respectively. Subsequently, further delaying the injection timing of methanol from 150 °CA to 80 °CA bTDC led to a decrease in combustion duration of 13.11% for pure methanol and a reduction by 54.11%, 43.51%, and 42.45% for methanol with 3%, 9%, and 12% hydrogen addition respectively. Shortest combustion duration was obtained when methanol was injected at 80°CA bTDC, this could relate to better evaporation and mixing before the start of ignition when compared to earlier injection timings of 150°CA and 110°CA bTDC of methanol as shown in

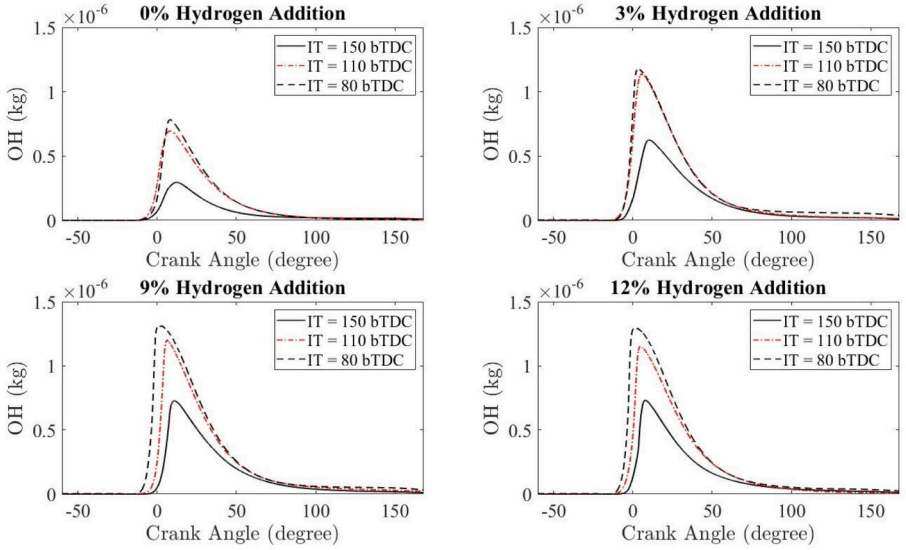

Fig. 9. The OH formation at different injection timings and hydrogen additions with respect to crank angle (ST = 20 °CA bTDC, Φ = 0.71, CR = 9.6, MAP = 90 kPa, N = 1200 rpm).

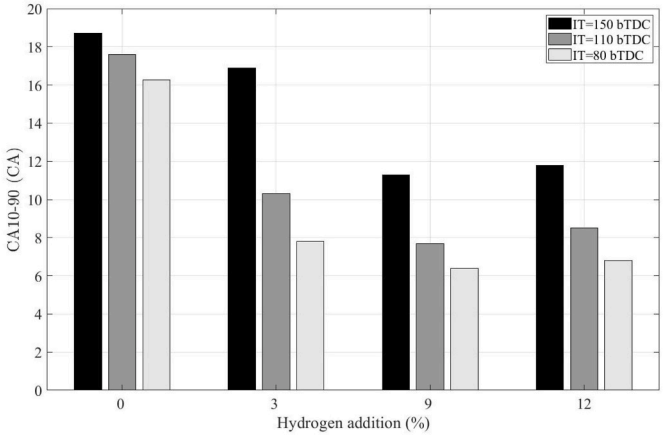

Fig. 10. Combustion duration CA10-90 at different injection timings and hydrogen additions (ST = 20 °CA bTDC, Φ = 0.71, CR = 9.6, MAP = 90 kPa, N = 1200 rpm).

Fig. 6. In addition to that it can be seen that by increasing hydrogen by 3%, 9% and 12%, the combustion duration (CA10-90) effectively reduces when compared to neat methanol for all the injection timing presented in this study. At an injection timing of 150 °CA bTDC, combustion duration decreased by 9.74%, 39.64%, and 36.98% for 3%, 9%, and 12% hydrogen addition compared to pure methanol, respectively. Similarly, at an injection timing of 110 °CA bTDC, combustion duration decreases by 41.50%, 56.42%, and 51.73% for 3%, 9%, and 12% hydrogen addition compared to pure methanol, respectively. Moreover, at an injection timing of 80 °CA bTDC, combustion duration decreases by 52.68%, 60.75%, and 58.26% for 3%, 9%, and 12% hydrogen addition compared to pure methanol. The observed variation is due to higher diffusivity of hydrogen that significantly enhances the formation of a favourable reactive mixture and the associated higher flame speed of hydrogen that fastens combustion. Fig. 10 also illustrates that for hydrogen addition beyond 9% resulted in an increase in combustion duration by 4.40%, 10.77% and 6.34% for retarded injection timing of 150 °CA bTDC, 110 °CA bTDC and 80 °CA bTDC respectively. This was mainly due to partial replacement of air under higher percentages of hydrogen addition that resulted in reducing the volumetric efficiency and flame propagation rate, similar kind of results were also observed in the experimental study of [49].

3.5. Emissions characteristics

The simulated results for NOx, Soot, and CO emissions from hydrogen-enriched methanol SI engine are discussed at different timings of methanol injection for varying percentages of hydrogen addition.

3.5.1. NOx emissions

Several studies have shown that enriching SI engines with hydrogen can lead to higher NOx emissions [55]. Fig. 11 shows the variation of NOx emission for 0%, 3%, 9% and 12% hydrogen addition at different injection timing of 150°CA, 120°CA and 80°CA bTDC, it can be seen that NOx emission increases respectively for the chosen conditions mentioned above. For neat methanol operating conditions, retarding the injection timing from 150 to 110 °CA bTDC resulted in the 161.37% increase in indicated specific NOx emission. Injection of methanol at 150 °CA bTDC resulted in a non-uniform mixture due to poor evaporation and wall film formation. Fig. 9 shows a reduction in the OH radical concentration and a reduction in the global combustion temperature

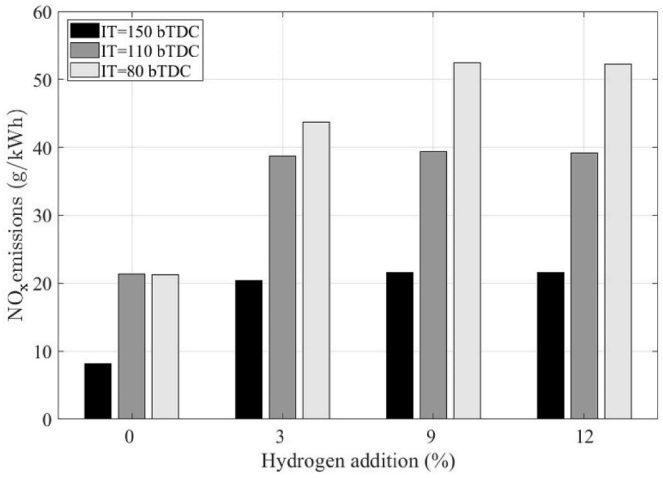

Fig. 11. Results for NOx emission for hydrogen addition ranging from 0 to 12% and injection timings from 150 to 80 °CA bTDC at a fixed spark timing (Φ = 0.71, CR = 9.6, MAP = 90 kPa, N = 1200 rpm).

contributing to lower NOx emissions, similar observations have also been reported in Ref. [56]. At an injection timing of 150°CA bTDC, the addition of 3%, 9%, and 12% hydrogen with methanol resulted in an increase in the magnitude of NOx emission by 149.13%, 164.90%, and 164.56%, respectively, compared to pure methanol. For the retarded injection timing of 110°CA bTDC, the addition of 3%, 9%, and 12% hydrogen resulted in an increase in NOx emission by 81.17%, 84.45%, and 83.41%, respectively, compared to pure methanol. Retarding the injection timing to 80°CA bTDC, resulted in an increase in NOx emission by 105.13%, 146.28%, and 145.06% for 3%, 9%, and 12% hydrogen addition, respectively, compared to pure methanol, as illustrated in Fig. 11. This is due to faster flame speed and higher adiabatic temperatures of hydrogen which also increases the in-cylinder temperature [57]. For methanol with 3%, 9% and 12% hydrogen addition under retarded injection timings of 150°CA bTDC to 110°CA bTDC resulted in 90%, 81.00% and 81.2% increase of NOx emissions. Retarding the injection timing further from 150°CA bTDC to 80°CA bTDC on methanol for 3%,9% and 12% hydrogen addition resulted in an increase in NOx emissions by 114.62%, 142.3% and 141.445% respectively. This was due to an increase in the peak in-cylinder pressure as shown in Fig. 5 which eventually leads to an increase in the in-cylinder temperature which increases NOx emissions. Additionally, the combustion duration was observed to decrease with hydrogen addition under in all tested conditions, as depicted in Fig. 10. This reduction in combustion duration indicates a clear trade-off, as rapid combustion could potentially contribute to the enhancement of thermal NO [58]. For 12% hydrogen addition there was a small reduction in NOx emission compared to 9% hydrogen for the injection timing of 150 °CA, 110 °CA and 80 °CA bTDC by 0.13%, 0.56% and 0.49%, respectively. This is due to reduction in lower oxygen concentration inside the cylinder due to higher percentage of hydrogen displacing air, similar effects were reported experimentally in Ref. [28].

3.5.2. Soot emissions

Fig. 12 shows the indicated specific soot emission of neat methanol and methanol with 3%, 9% and 12% hydrogen addition for injection timings of methanol at 150 °CA bTDC,110 °CA bTDC and 80 °CA bTDC at a fixed spark timing of 20 °CA bTDC. The addition of hydrogen to methanol consistently reduced soot emissions at various injection timings compared to neat methanol. Fig. 12 illustrates a decrease in indicated specific soot emissions when injection timing was retarded from 150 °CA bTDC to 110 °CA bTDC a considerable decrease of up to 93%, 97%, 98% and 94% was observed for corresponding hydrogen addition levels of 0%, 3%, 9% and 12% respectively. Similarly, Fig. 12 also demonstrates a decrease in indicated specific soot emissions with the retardation of injection timing from 150 °CA bTDC to 80 °CA bTDC, with the soot emissions following a declining pattern of 98%, 98%, 98%, 99% for corresponding hydrogen addition levels of 0%, 3%, 9% and 12% respectively. Specifically, at an injection timing of 150 °CA bTDC a reduction of 63.4%, 76.9%, and 61.90% of soot were observed of 3%, 9% and 12% hydrogen when compared to neat methanol. At 110 °CA bTDC, reduction of indicated soot emission obtained for 3%, 9% and 12% hydrogen addition of methanol was 84.24%, 93.55%, and 64.4%, and at 80 °CA bTDC, reductions were 67%, 82.4%, and 78.9%, respectively, compared to neat methanol. This reduction in soot could be related to higher OH radical concentration with hydrogen addition in methanol compared to neat methanol as can be seen in Fig. 9. The OH radical play a crucial role in enhancing the soot oxidation process during combustion [30]. In addition, it was also observed that from Fig. 12 the indicated specific NOx emission was higher for methanol with hydrogen addition compared to neat methanol, and the trend is contrary for soot which is the clear trade-off, The addition of hydrogen facilitates and rapid due to higher burning flame speed [59]. Since there is no carbon-carbon chain and lack of any aromatic content the overall amount of soot produced from methanol combustion is negligible. The presence of hydroxyl group also favours oxidation through a maximum reduction of up to 99% has been obtained the actual magnitude variations between the operating conditions are insignificant therefore a semi-log scale was used to highlight the differences. Hydrogen addition greater than 9% resulted in a rise in soot emissions for all injection timings because of the depletion of oxygen content in the cylinder.

3.5.3. Indicated specific CO emissions

The results of Indicated specific CO emission represent the effect of incomplete combustion [17,19,28,60]. Fig. 13 shows that the indicated specific CO emission for methanol combustion for varying percentages of hydrogen addition to methanol for different injection timings at 150°CA, 110°CA and 80 °CA bTDC at fixed spark timing of 20 °CA bTDC. High indicated specific CO emission was observed when methanol was injected at 150 °CA bTDC under all concentration of hydrogen additions with methanol compared to injection timing of 110 ° CA bTDC and 80 °CA bTDC. This could be due to poor evaporation leading to formation of liquid film on piston crown and accumulation of rich fuel-air mixture as discussed in Figs. 6–7 also leads to an increase in CO emission. Through the amount of methanol injection was reduced with hydrogen addition the above-mentioned effect was still present for 150° CA bTDC compared to retarded injection timing. In addition to that it was also evident that the formation of OH radical at 150 °CA bTDC injection

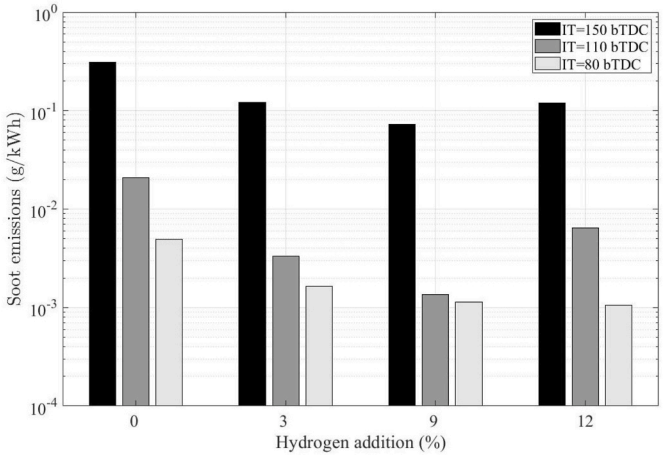

Fig. 12. Indicated specific soot emission for hydrogen addition ranging from 0 to 12 % and injection timings from 150 °CA to 80 °CA bTDC at a fixed spark timing (Φ = 0.71, CR = 9.6, MAP = 90 kPa, N = 1200 rpm).

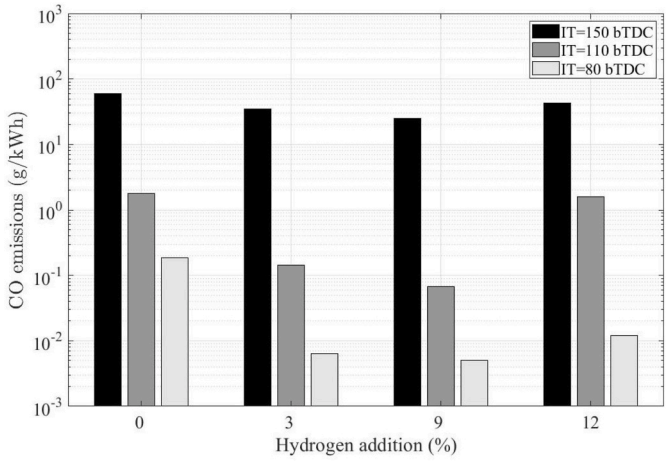

Fig. 13. Results for CO emission for hydrogen addition ranging from 0 to 12 % and injection timings from 150 to 80 °CA bTDC at a fixed spark timing (Φ = 0.71, CR = 9.6, MAP = 90 kPa, N = 1200 rpm).

timing was lower compared to 110 °CA and 80 °CA bTDC that resulted in partial oxidation of fuel. It was also observed that retarding the injection timing from 150 °CA bTDC to 110°CA bTDC and 80°CA bTDC for (0%, 3%, 9% and 12%) hydrogen additions to methanol caused the indicated specific CO emission to decrease significantly hence they are presented on a semi-log plot in Fig. 13. The addition of hydrogen to methanol at various concentrations resulted in a consistent reduction in specific CO emissions compared to using pure methanol across different injection timings. For the injection timing of 150 °CA bTDC, the addition of 3%, 9%, and 12% hydrogen lowered CO emissions to 41.78%, 58.21%, and 28.59%, respectively, compared to neat methanol. Significant reductions were observed at injection timings of 110 °CA bTDC and 80 °CA bTDC. Furthermore, compared to 9% hydrogen addition with methanol, the addition of 12% hydrogen with methanol resulted in 41.48%, 95.72%, and 58.10% rise in indicated specific CO emissions for injection timings of 150, 110, and 80 °CA bTDC. This could be due to fixed global equivalence ratio operation, so any further addition of hydrogen beyond 9% lowers the oxidation potential of the in-cylinder mixture during combustion which also affects the volumetric efficiency. The outcomes of CO emission from this simulation work are in agreement with experimental findings presented in Ref. [24].

3.5.4. Indicated specific HC emissions

Fig. 14 shows the indicated specific hydrocarbon (HC) emissions for a hydrogen-enriched methanol spark-ignition (SI) engine at various percentages of hydrogen addition and injection timings of 150, 110, and 80 °CA bTDC. It is evident that the injection timing of 150 °CA bTDC resulted in the highest indicated specific HC emissions across all hydrogen addition levels compared to 110 °CA bTDC and 80 °CA bTDC. This may be due to inadequate evaporation, leading to the formation of a liquid film on the piston crown and a build-up of a methanol-rich fuel-air mixture, as previously mentioned in Figs. 6 and 7. Wall wetting in the combustion chamber can cause unburned hydrocarbon emissions [61]. Moreover, it was observed that retarding the injection timing from 150 °CA to 110 °CA and 80 °CA bTDC significantly reduced the indicated specific HC emissions, as illustrated in the semi-log plot in Fig. 14. The addition of 3%, 9%, and 12% hydrogen to methanol consistently reduced the indicated specific HC emissions compared to neat methanol at all injection timings. This could be attributed to the reduction in exhaust temperature [24]. However, hydrogen additions greater than 9% resulted in a slight increase in indicated specific HC emissions across all injection timings (150 °CA, 110 °CA, and 80 °CA bTDC). This may be due to higher hydrogen concentrations impacting volumetric efficiency and reducing the oxidation process, as noted in previous experimental findings [24].

4. Conclusions

The effect of injection timing on the performance and emissions of a hydrogen enriched methanol SI engine was evaluated by using the three-dimensional computational fuel dynamics model. Increasing the percentage of hydrogen in the mixture resulted in an earlier rise of in-cylinder pressure as well as increased the maximum in-cylinder pressure compared to neat methanol operation and this effect was observed only up to 9% Hydrogen enrichment, beyond which the peak values of the in-cylinder pressure decreased due to reduction in the overall energy content of the charge. The magnitude of OH radicals formed during the combustion process also increased with hydrogen enrichment. For all the considered injection timings of methanol, the combustion duration reduced up to 9% enrichment of hydrogen beyond which it increased and a similar trend was observed for carbon monoxide, unburnt hydrocarbon and soot emissions but the overall magnitude of soot was insignificant. The NOx emissions increased with the addition of hydrogen of up to 9% in the mixture and thereafter it maintained a plateau. Enrichment of hydrogen favoured ignition under late injection of up to 60 °CA bTDC in neat methanol operation. The outcome of this study has shown that the enrichment of hydrogen in a methanol SI engine favours ignition but the performance benefits are limited with higher percentages of hydrogen in this mode of operation.

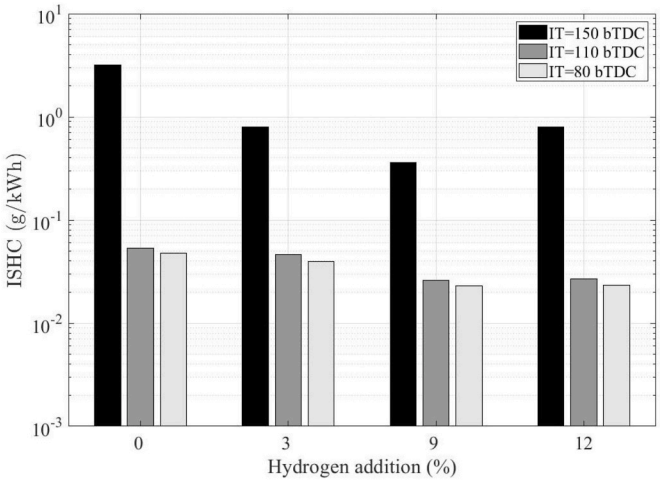

Fig. 14. Indicated specific HC emissions at various injection timing and hydrogen additions.

CRediT authorship contribution statement

S.N. Iyer: Writing – original draft, Visualization, Software, Methodology, Investigation, Conceptualization. **D.N. Rrustemi:** Visualization, Validation, Methodology, Investigation. **L.C. Ganippa:** Writing – review & editing, Supervision, Methodology. **T. Megaritis:** Writing – review & editing, Supervision, Methodology.

Declaration of competing interest

The authors declare that they have no known competing financial interests or personal relationships that could have appeared to influence the work reported in this paper.

Acknowledgements

Convergent Science provided CONVERGE licenses and technical support for this work.

References

[1] Sahu S, Kumar P, Dhar A. Effect of injection timing on combustion, performance and emissions characteristics of methanol fuelled DISI engine: a numerical study. Fuel 2022;322:124167. https://doi.org/10.1016/j.fuel.2022.124167.
[2] Azhari NJ, Erika D, Mardiana S, Ilmi T, Gunawan ML, Makertihartha IGBN, et al. Methanol synthesis from CO2: a mechanistic overview. Results Eng 2022;16:100711. https://doi.org/10.1016/j.rineng.2022.100711.
[3] Jadhav SG, Vaidya PD, Bhanage BM, Joshi JB. Catalytic carbon dioxide hydrogenation to methanol: a review of recent studies. Chem Eng Res Des 2014;92:2557–67. https://doi.org/10.1016/j.cherd.2014.03.005.
[4] Verhelst S. Recent progress in the use of hydrogen as a fuel for internal combustion engines. Int J Hydrogen Energy 2014;39:1071–85. https://doi.org/10.1016/j.ijhydene.2013.10.102.
[5] García-Freites S, Gough C, Röder M. The greenhouse gas removal potential of bioenergy with carbon capture and storage (BECCS) to support the UK's net-zero emission target. Biomass Bioenergy 2021;151:106164. https://doi.org/10.1016/j.biombioe.2021.106164.
[6] Mishra PC, Gupta A, Kumar A, Bose A. Methanol and petrol blended alternate fuel for future sustainable engine: a performance and emission analysis. Measurement 2020;155:107519. https://doi.org/10.1016/j.measurement.2020.107519.
[7] Verhelst S, Turner JW, Sileghem L, Vancoillie J. Methanol as a fuel for internal combustion engines. Prog Energy Combust Sci 2019;70:43–88. https://doi.org/10.1016/j.pecs.2018.10.001.
[8] Turner JWG, Pearson RJ, Holland B, Peck R. Alcohol-based fuels in high performance engines. 2007-01–0056, https://doi.org/10.4271/2007-01-0056; 2007.

[9] Nguyen D-K, Sileghem L, Verhelst S. Exploring the potential of reformed-exhaust gas recirculation (R-EGR) for increased efficiency of methanol fueled SI engines. Fuel 2019;236:778–91. https://doi.org/10.1016/j.fuel.2018.09.073.

[10] Yilmaz N. Comparative analysis of biodiesel–ethanol–diesel and biodiesel–methanol–diesel blends in a diesel engine. Energy 2012;40:210–3. https://doi.org/10.1016/j.energy.2012.01.079.

[11] Wei Y, Liu S, Liu F, Liu J, Zhu Z, Li G. Formaldehyde and methanol emissions from a methanol/gasoline-fueled spark-ignition (SI) engine. Energy Fuels 2009;23:3313–8. https://doi.org/10.1021/ef900175h.

[12] Rrustemi DN, Ganippa LC, Axon CJ. Investigation of boost pressure and spark timing on combustion and NO emissions under lean mixture operation in hydrogen engines. Fuel 2023;353:129192. https://doi.org/10.1016/j.fuel.2023.129192.

[13] Wang J, Chen H, Liu B, Huang Z. Study of cycle-by-cycle variations of a spark ignition engine fueled with natural gas–hydrogen blends. Int J Hydrogen Energy 2008;33:4876–83. https://doi.org/10.1016/j.ijhydene.2008.06.062.

[14] Bhasker JP, Porpatham E. Effects of compression ratio and hydrogen addition on lean combustion characteristics and emission formation in a Compressed Natural Gas fuelled spark ignition engine. Fuel 2017;208:260–70. https://doi.org/10.1016/j.fuel.2017.07.024.

[15] Wang X, Zhang H, Yao B, Lei Y, Sun X, Wang D, et al. Experimental study on factors affecting lean combustion limit of S.I engine fueled with compressed natural gas and hydrogen blends. Energy 2012;38:58–65. https://doi.org/10.1016/j.energy.2011.12.042.

[16] Gong C-M, Huang K, Jia J-L, Su Y, Gao Q, Liu X-J. Improvement of fuel economy of a direct-injection spark-ignition methanol engine under light loads. Fuel 2011;90:1826–32. https://doi.org/10.1016/j.fuel.2010.10.032.

[17] Gong C, Li Z, Sun J, Liu F. Evaluation on combustion and lean-burn limit of a medium compression ratio hydrogen/methanol dual-injection spark-ignition engine under methanol late-injection. Appl Energy 2020;277:115622. https://doi.org/10.1016/j.apenergy.2020.115622.

[18] Gong C, Li Z, Yi L, Huang K, Liu F. Research on the performance of a hydrogen/methanol dual-injection assisted spark-ignition engine using late-injection strategy for methanol. Fuel 2020;260:116403. https://doi.org/10.1016/j.fuel.2019.116403.

[19] Gong C-M, Huang K, Jia J-L, Su Y, Gao Q, Liu X-J. Regulated emissions from a direct-injection spark-ignition methanol engine. Energy 2011;36:3379–87. https://doi.org/10.1016/j.energy.2011.03.035.

[20] Gong C, Li Z, Liu F. Numerical study of the firing, radicals and intermediates in the combustion process of a H2-assisted combustion DISI methanol engine. Fuel 2023;348:128603. https://doi.org/10.1016/j.fuel.2023.128603.

[21] Kanth S, Debbarma S. Comparative performance analysis of diesel engine fuelled with hydrogen enriched edible and non-edible biodiesel. Int J Hydrogen Energy 2021;46:10478–93. https://doi.org/10.1016/j.ijhydene.2020.10.173.

[22] Nuthan Prasad BS, Pandey JK, Kumar GN. Effect of hydrogen enrichment on performance, combustion, and emission of a methanol fueled SI engine. Int J Hydrogen Energy 2021;46:25294–307. https://doi.org/10.1016/j.ijhydene.2021.05.039.

[23] Zhang B, Ji C, Wang S, Liu X. Combustion and emissions characteristics of a spark-ignition engine fueled with hydrogen–methanol blends under lean and various loads conditions. Energy 2014;74:829–35. https://doi.org/10.1016/j.energy.2014.07.055.

[24] Gong C, Li Z, Chen Y, Liu J, Liu F, Han Y. Influence of ignition timing on combustion and emissions of a spark-ignition methanol engine with added hydrogen under lean-burn conditions. Fuel 2019;235:227–38. https://doi.org/10.1016/j.fuel.2018.07.097.

[25] Wei M, Liu J, Guo G, Li S. The effects of hydrogen addition on soot particle size distribution functions in laminar premixed flame. Int J Hydrogen Energy 2016;41:6162–9. https://doi.org/10.1016/j.ijhydene.2015.10.022.

[26] Gong C, Li Z, Yi lin, Huang K, Liu F. Research on the performance of a hydrogen/methanol dual-injection assisted spark-ignition engine using late-injection strategy for methanol. Fuel 2020;260:116403. https://doi.org/10.1016/j.fuel.2019.116403.

[27] Ji C, Zhang B, Wang S. Enhancing the performance of a spark-ignition methanol engine with hydrogen addition. Int J Hydrogen Energy 2013;38:7490–8. https://doi.org/10.1016/j.ijhydene.2013.04.001.

[28] Gong C, Li Z, Chen Y, Liu J, Liu F, Han Y. Influence of ignition timing on combustion and emissions of a spark-ignition methanol engine with added hydrogen under lean-burn conditions. Fuel 2019;235:227–38. https://doi.org/10.1016/j.fuel.2018.07.097.

[29] Jose J, Parsi A, Shridhara S, Mittal M, Ramesh A. Effect of fuel injection timing on the mixture preparation in a small gasoline direct-injection engine. 2018-32–0014, https://doi.org/10.4271/2018-32-0014; 2018.

[30] Zhang Y, Wang Q, Yang R, Yan Y, Fu J, Liu Z. Numerical investigation of the effect of injection timing on the in-cylinder activity of a gasoline direct injection engine. Adv Mech Eng 2022;14:168781322210828. https://doi.org/10.1177/16878132221082873.

[31] Yan Y, Yang R, Sun X, Li R, Liu Z. Numerical investigations of injection timing effects on a gasoline direct injection engine performance: Part A, in-cylinder combustion process. Front Energy Res 2022;10:828167. https://doi.org/10.3389/fenrg.2022.828167.

[32] Harshavardhan B, Mallikarjuna JM. Effect of piston shape on in-cylinder flows and air–fuel interaction in a direct injection spark ignition engine – a CFD analysis. Energy 2015;81:361–72. https://doi.org/10.1016/j.energy.2014.12.049.

[33] Mohammadi A, Shioji M, Nakai Y, Ishikura W, Tabo E. Performance and combustion characteristics of a direct injection SI hydrogen engine. Int J Hydrogen Energy 2007;32:296–304. https://doi.org/10.1016/j.ijhydene.2006.06.005.

[34] Al-Muhsen NFO, Huang Y, Hong G. Effects of direct injection timing associated with spark timing on a small spark ignition engine equipped with ethanol dual-injection. Fuel 2019;239:852–61. https://doi.org/10.1016/j.fuel.2018.10.118.

[35] Jiao Q, Reitz RD. The effect of operating parameters on soot emissions in GDI engines. SAE Int J Engines 2015;8:1322–33. https://doi.org/10.4271/2015-01-1071.

[36] Venugopal T, Ramesh A. Experimental studies on the effect of injection timing in a SI engine using dual injection of n-butanol and gasoline in the intake port. Fuel 2014;115:295–305. https://doi.org/10.1016/j.fuel.2013.07.013.

[37] Zhang B, Ji C, Wang S. Combustion analysis and emissions characteristics of a hydrogen-blended methanol engine at various spark timings. Int J Hydrogen Energy 2015;40:4707–16. https://doi.org/10.1016/j.ijhydene.2015.01.142.

[38] Lee J, Park C, Bae J, Kim Y, Choi Y, Lim B. Effect of different excess air ratio values and spark advance timing on combustion and emission characteristics of hydrogen-fueled spark ignition engine. Int J Hydrogen Energy 2019;44:25021–30. https://doi.org/10.1016/j.ijhydene.2019.07.181.

[39] Yilmaz İ, Taştan M. Investigation of hydrogen addition to methanol-gasoline blends in an SI engine. Int J Hydrogen Energy 2018;43:20252–61. https://doi.org/10.1016/j.ijhydene.2018.07.088.

[40] Yu X, Hu Z, Guo Z, Li D, Wang T, Li Y, et al. Research on combustion and emission characteristics of a hydrous ethanol/hydrogen combined injection spark ignition engine under lean-burn conditions. Int J Hydrogen Energy 2022;47:27223–36. https://doi.org/10.1016/j.ijhydene.2022.06.046.

[41] Wang S, Ji C, Zhang B. Starting a spark-ignited engine with the gasoline–hydrogen mixture. Int J Hydrogen Energy 2011;36:4461–8. https://doi.org/10.1016/j.ijhydene.2011.01.020.

[42] Gong C, Li Z, Yi L, Liu F. Experimental investigation of equivalence ratio effects on combustion and emissions characteristics of an H2/methanol dual-injection engine under different spark timings. Fuel 2020;262:116463. https://doi.org/10.1016/j.fuel.2019.116463.

[43] Richards KJ, Senecal PK, Pomraning E. Converge 3.1. 2024.

[44] Yakhot V, Orszag SA. Renormalization group analysis of turbulence. I. Basic theory. J Sci Comput 1986;1:3–51. https://doi.org/10.1007/BF01061452.

[45] Lorenzzetti GS, Vaz FA, De Bortoli ÁL. Development of reduced reaction mechanisms for hydrogen and methanol diffusion flames. Math Comput Model 2013;57:2316–24. https://doi.org/10.1016/j.mcm.2011.08.049.

[46] Senecal PK, Pomraning E, Richards KJ, Briggs TE, Choi CY, Mcdavid RM, et al. Multi-dimensional modeling of direct-injection diesel spray liquid length and flame lift-off length using CFD and parallel detailed. Chemistry 2003. https://doi.org/10.4271/2003-01-1043. 2003-01–1043.

[47] Cheng X, Jv H, Wu Y. Application of a phenomenological soot model for diesel engine combustion. In: ASME 2008 intern. Combust. Engine Div. Spring Tech. Conf. Chicago, Illinois, USA: ASMEDC; 2008. p. 205–14. https://doi.org/10.1115/ICES2008-1629.

[48] Liu X, Ji C, Gao B, Wang S, Liang C, Yang J. A laminar flame speed correlation of hydrogen–methanol blends valid at engine-like conditions. Int J Hydrogen Energy 2013;38:15500–9. https://doi.org/10.1016/j.ijhydene.2013.09.031.

[49] Purayil STP, Hamdan MO, Al-Omari SAB, Selim MYE, Elnajjar E. Review of hydrogen–gasoline SI dual fuel engines: engine performance and emission. Energy Rep 2023;9:4547–73. https://doi.org/10.1016/j.egyr.2023.03.054.

[50] Montanaro A, Malaguti S, Alfuso S. Wall impingement process of a multi-hole GDI spray: experimental and numerical investigation. 2012-01–1266, https://doi.org/10.4271/2012-01-1266; 2012.

[51] Kim T, Song J, Park J, Park S. Numerical and experimental study on effects of fuel injection timings on combustion and emission characteristics of a direct-injection spark-ignition gasoline engine with a 50 MPa fuel injection system. Appl Therm Eng 2018;144:890–900. https://doi.org/10.1016/j.applthermaleng.2018.09.007.

[52] Schlapbach L, Züttel A. Hydrogen-storage materials for mobile applications. Mater. Sustain. Energy 2010:265–70. https://doi.org/10.1142/9789814317665_0038. Co-Published with Macmillan Publishers Ltd, UK.

[53] Xiao P, Lee C, Wu H, Akram MZ, Liu F. Impacts of hydrogen-addition on methanol-air laminar burning coupled with pressures variation effects. Energy 2019;187:115997. https://doi.org/10.1016/j.energy.2019.115997.

[54] Zhang R, Chen L, Wei H, Pan J, Li J, Yang P, et al. Optical study on the effects of the hydrogen injection timing on lean combustion characteristics using a natural gas/hydrogen dual-fuel injected spark-ignition engine. Int J Hydrogen Energy 2021;46:20777–89. https://doi.org/10.1016/j.ijhydene.2021.03.171.

[55] Park C, Lim G, Lee S, Kim C, Choi Y. Effects of the ignition timing retard and the compression ratio on the full-load performance and the emissions characteristics of a heavy-duty engine fuelled by hydrogen–natural-gas blends. Proc Inst Mech Eng Part J Automob Eng 2013;227:1295–302. https://doi.org/10.1177/0954407013495528.

[56] Jesu Godwin D, Edwin Geo V, Thiyagarajan S, Leenus Jesu Martin M, Maiyalagan T, Saravanan CG, et al. Effect of hydroxyl (OH) group position in alcohol on performance, emission and combustion characteristics of SI engine. Energy Convers Manag 2019;189:195–201. https://doi.org/10.1016/j.enconman.2019.03.063.

[57] Huang F, Kong W. Effects of hydrogen addition on combustion characteristics of a free-piston linear engine with glow-assisted ignition. Int J Hydrogen Energy 2021;46:23040–52. https://doi.org/10.1016/j.ijhydene.2021.04.093.

[58] Kesgin U. Study on prediction of the effects of design and operating parameters on NOx emissions from a leanburn natural gas engine. Energy Convers Manag 2003;44:907–21. https://doi.org/10.1016/S0196-8904(02)00093-6.

[59] Gong C, Li Z, Yi lin, Huang K, Liu F. Research on the performance of a hydrogen/methanol dual-injection assisted spark-ignition engine using late-injection strategy

for methanol. Fuel 2020;260:116403. https://doi.org/10.1016/j.fuel.2019.116403.
[60] Gong C, Li D, Li Z, Liu F. Numerical study on combustion and emission in a DISI methanol engine with hydrogen addition. Int J Hydrogen Energy 2016;41:647–55. https://doi.org/10.1016/j.ijhydene.2015.11.062.
[61] Verhelst S, Turner JW, Sileghem L, Vancoillie J. Methanol as a fuel for internal combustion engines. Prog Energy Combust Sci 2019;70:43–88. https://doi.org/10.1016/j.pecs.2018.10.001.